Phytochemicals and micronutrients in suppressing infectivity caused by SARS-CoV-2 virions and seasonal coronavirus HCoV-229E *in vivo*

ANNA GOC, WALDEMAR SUMERA, MATTHIAS RATH and ALEKSANDRA NIEDZWIECKI* ⓘD

Dr. Rath Research Institute, 5941 Optical CT, San Jose, CA-95138, USA

ORIGINAL RESEARCH PAPER

ABSTRACT

SARS-CoV-2 infection still poses health threats especially to older and immunocompromised individuals. New emerging variants of SARS-CoV-2, including Omicron and Arcturus, have been challenging the effectiveness of humoral immunity resulting from repeated vaccination and infection. With recent study implying a wave of new mutants in vaccinated people making them more susceptible to the newest variants and fueling a rapid viral evolution, there is a need for alternative or adjunct approaches against coronavirus infections other than vaccines. Our earlier work indicated that a specific combination of micronutrients and phytochemicals can inhibit key infection mechanisms shared by SARS-CoV-2 and its variants *in vitro*. Here we demonstrate *in vivo* that an intake of this micronutrient combination before and during infection of mice with engineered SARS-CoV-2 virions and HCoV-229E virus results in a significant decrease in viral load and level of spike protein in the lungs. This was accompanied by decreased inflammatory response, including TNFα, IL1β, ILα, and IL17. These and our earlier results confirm that by targeting multiple mechanisms simultaneously by a combination treatment we can effectively and safely challenge SARS-CoV-2 and HCoV-229E virus. If clinically confirmed, such an approach could complement already in-use preventive and therapeutic strategies against coronavirus infections.

INTRODUCTION

As of February 19, 2023, over 757 million confirmed cases and over 6.8 million deaths due to COVID-19 have been reported globally [1]. It was also stated that since 2022 incidence rates are decreasing overall, but the threat of COVID-19 is still strong in some groups of people, i.e., the elderly and individuals with morbidities such as impaired immunity. The observations that RNA/DNA-based treatments, i.e., vaccines and drugs, offer little or no protection against preventing infections and transmission of SARS-CoV-2 and its variants raised concerns that current vaccination programs are not fully effective against new variants [2]. Variants of SARS-CoV-2, Omicron BA.1, BA.2, and BA.5, have demonstrated strong evasion capability, posing severe challenges to the effectiveness of humoral immunity established through vaccination and infection [3–9]. Moreover, recent study implies an increasing wave of new mutants in vaccinated individuals as repeated vaccinations may make people more susceptible to the newest variants and fuel rapid evolution of the virus [10].

In a search for an alternative or an adjunct approach to already applied treatments and medications against coronaviruses, including those requiring adjustments for any new viral

*Corresponding author.
E-mail: author@drrath.com

AKJournals

mutations, we turned to explore natural compounds known for their anti-viral effects. Based on experimental testing we developed a combination of compounds that can simultaneously affect several key mechanisms associated with SARS-CoV-2 infection. We have shown that a combination of vitamin C with polyphenols and other micronutrients can suppress cellular mechanisms associated with cellular entry and processing of SARS-CoV-2 including its Alpha, Beta, Delta, Kappa, Mu, and Omicron variants [11]. Efficacy of this composition against RNA-dependent RNA polymerase (RdRp) complex (nsp12/nsp7/nsp8) of both SARS-CoV-2 and Omicron variants would signal a possibility of the application of these compounds, as a single combination, in controlling RdRp activity across a wider spectrum of viral species [12]. In addition, this complex could inhibit spike protein binding to receptor binding domain (RBD) of SARS-CoV-2 and its mutated forms, including their cellular entry, as well as angiotensin-converting enzyme 2 receptor (ACE2) expression at the protein and RNA levels. Particularly significant was the fact that this inhibitory effect on ACE2 molecule was maintained even under pro-inflammatory conditions [13–15].

In this study, we tested the effects of this composition *in vivo* on the viral load as well as spike protein levels in the lungs of infected mice. The animals were infected and re-infected with engineered SARS-CoV-2 virions (SARS-CoV-2 as rVSVΔG-SARS-CoV-2-S-D614GΔ21-NLucP) as well as with the seasonal coronavirus HCoV-229E, in order to evaluate its universality and potential applicability against various human coronavirus strains.

MATERIALS AND METHODS

Viral particles and antibodies

Human coronavirus 229E (HCoV-229E) was obtained from ATCC (American Type Culture Collection) (Manassas, VA, USA) and maintained in Modified Eagle's Medium containing 10% fetal bovine serum. Replication-competent SARS-CoV-2 as rVSVΔG-SARS-CoV-2-S-D614GΔ21-NLucP was purchased from Kerafast (Boston, MA, USA). rVSVΔG-SARS-CoV-2-S-D614Gd21-NLucP is a recombinant vesicular stomatitis virus, in which the native glycoprotein has been replaced with the SARS-CoV-2 spike protein lacking the last 21 residues of the cytoplasmic tail and contains the D614G amino acid change (SMet1D614GΔ21), thus the virus is capable of interacting and entering cells through the SARS-CoV-2 spike, but once fusion occurs, it replicates using the vesicular stomatitis virus (VSV) machinery. This virus also encodes nano-luciferase PEST (nLucP) to enable easy quantification of viral replication. SARS-CoV-2 anti-spike antibody was purchased from GeneTex (Irvine, CA, USA), whereas, anti-CD11b antibody and anti-β-actin antibody were obtained from Cell Signaling (Danvers, MA, USA). HCoV-229E anti-spike antibody was acquired from R&D Systems (Minneapolis, MN, USA). SARS-CoV-2 viral like particles (VLPs) were obtained from Creative Biostructure (Shirley, NY, USA).

MixV composition

The combination of natural compounds (MixV) tested in this study is presented in Table 1. Stock solution of this combination was prepared in DMSO at 50 mg ml^{-1}. Concentration of each individual compound accounted for 4.44 mg/mouse.

NF-κB activity assay

NF-κB activity was performed according to the Indigo Biosciences assay kit (State College, PA, USA). Briefly, 21 ml suspension of reporter cells was distributed into 96-well plates (200 μl per well) and pre-incubated in 37 °C at 5% CO_2 for 5 h. Next, the medium was removed, cells were rinsed with Cell Screening Medium (CSM) and replaced with stock solution of MixV diluted with CSM to 10 μg ml^{-1} concentration. SARS-CoV-2 VLPs (with properties of inducing immune responses) were used at 5 μg ml^{-1}, and 'no treatment' control was included as well. The plates were kept in 37 °C at 5% CO_2 for 23 h. Next, the treatment medium was discarded and 100 μl of Luciferase Detection Reagent (LDR) was added to each well of the assay plate. After 5 min, chemiluminescence was measured. Results are expressed as a percentage of composition-free control (mean $\pm$ standard deviation (SD), $n = 4$).

Cytokines ELISA assays

Pro-inflammatory cytokines and chemokines release was assessed using the Mouse Cytokines ELISA array assay kit (Signosis, Santa Clara, CA, USA) according to the manufacturer's protocol. Briefly, 100 μl of bronchoalveolar lavage (BAL) was incubated for 2 h in 96-well plates at room temperature with gentle shaking. Next, all wells were washed three times with 1 × Assay Wash Buffer and again incubated with 100 μl of biotin-labeled antibody mixture for 1 h at room temperature with gentle shaking. The washing step was then repeated and all wells were again incubated with streptavidin-HRP conjugated for 45 min at room temperature with gentle shaking followed by one more washing step. Signal was developed with TMB substrate followed by adding a stop solution. Optical density was measured within 30 min at 450 nm. Results are expressed as a percentage of composition-free control (mean $\pm$ SD, $n = 4$).

Table1. Composition of the test MixV

Compound
Curcumin
Theaflavin 3,3′ digallate
Quercetin
Baicalin
Resveratrol
Naringenin
NAC

In vivo study

6-8 week-old K18-hACE2 C57BL/6J mice weighing approximately 20–25 g were used in this study (The Jackson Laboratory, Bar Harbor, ME, USA). The mice were kept at an ambient temperature of 21 °C with standard rodent diet and water provided *ad libitum* during a light and dark cycle of 12 h. Mice were randomly divided into five experimental groups: uninfected animals were gavaged with 1.0% ethanol, intra-tracheally infected animals with 1.0% ethanol, uninfected animals with 100 mg/kg MixV, and intra-tracheally infected animals with 100 mg/kg MixV. Either 1×10^5 tissue infectious doses ($TCID_{50}$) of HCoV-229E or 3×10^5 of tissue infectious dose ($TCID_{50}$) of rVSVΔG-SARS-CoV-2-S-D614Gd21-NLucP particles were inoculated intra-tracheally into animals from infected only and infected and treated experimental groups. Additionally, part of the animals from infected and infected and gavaged experimental groups were mid-term intra-tracheally re-infected with continued oral gavaging of MixV. Oral gavaging began 24 h prior to viral infection. At the end of the study all animals were sacrificed and the lung samples were collected for further testing. Weights of gavaged animals were measured daily. All animals were sacrificed by overdosing of isoflurane. Lung and BAL samples were collected, immediately snap-frozen in liquid nitrogen and subjected to RT-qPCR and/or ELISA assay. For histology/immunohistochemistry, tissues were fixed in 10% neutral-buffered formalin for 3 days and placed in 70% ethanol and stored until histology/immunohistochemistry was performed.

Quantification of RNA

rVSVΔG-SARS-CoV-2-S-D614Gd21-NLucP genome copies in lung tissues were quantified by extracting RNA with a Qiagen RNA Plus Isolation kit (Germantown, MD, USA), according to manufacturer's protocol. $2.0 \, \mu g \, ml^{-1}$ extracted RNA was then taken for cDNA synthesis using the High-Capacity RNA-to-cDNA kit following the manufacturer's protocol (Thermo Fisher, Waltham, MA, USA). Two-step RT-qPCR exploiting the TaqMan[TM] principle was then executed in triplicates for each sample using Vesicular Stomatitis Virus Polymerase (L) Gene[®] Genesig Advanced Kit (Primerdesign Ltd, Plymouth Meeting, PA, USA) and Bio-Rad CFX instrument (Hercules, CA), with cycling parameters as: 2 min at 95 °C; and 50 cycles at 95 °C for 10 s and 60 °C for 60 s. Viral copies of SARSCoV-2 were detected using primers for the L region of the VSV genome. Genomic copies per lung tissue were normalized to the relative expression of the mouse RNA Polymerase II gene (Pol2Ra) using TaqMan[TM]. Gene Expression Assays (Thermo Fisher, Waltham, MA, USA).

HCoV-229E genome copies in lung tissues were quantified by extracting RNA with a Qiagen RNA Plus Isolation kit (Germantown, MD, USA), according to the manufacturer's protocol. $2.0 \, \mu g \, ml^{-1}$ extracted RNA was then taken for cDNA synthesis using a High-Capacity RNA-to-cDNA kit, following the manufacturer's protocol (Thermo Fisher, Waltham, MA, USA). Two-step RT-qPCR with TaqMan[TM] Advanced Master Mix and TaqMan[TM] Gene Expression Assay (Thermo Fisher, Waltham, MA, USA) was then executed in triplicates for each sample on a BioRad CFX instrument (Hercules, CA), with cycling parameters as: 20 s at 95 °C; and 40 cycles at 95°C for 3 s and 60 °C for 30 s. Genomic copies per lung tissue were normalized to the relative expression of the mouse RNA Polymerase II gene (Pol2Ra) using TaqMan[TM].Gene Expression Assays (Thermo Fisher, Waltham, MA, USA).

Immunohistochemistry

Lung tissues were immediately fixed after harvesting, embedded in paraffin, subjected to sectioning (5 μm sections), and stained with hematoxylin and eosin (H&E) as well as with antibodies against SARS-CoV-2 spike protein and CD11b (pan myeloid cells), respectively. For H&E staining, lung sections were processed following standard histological procedure. For indirect immunohistochemistry (IHC), lung sections were also processed following standard immuno-histochemical technique with antigen retrieval (i.e., 15 min heat-induced with EDTA pH 6.0). Primary antibodies were used as follows: anti-spike protein at 1:200 dilution and anti-CD11b at 1:200 dilution. Images taken were scanned with the Aperio AT2 system (Leica, Buffalo Grove, IL). The areas with detected spike protein and CD11b were divided by the sum of the areas corresponding to cellular structures counterstained with hematoxylin + anti-spike protein and anti-CD11b, respectively. Calculated ratios are represented as a percentage of control. All histology and IHC was performed - by a third party at the Inotiv facility (Boulder, CO, USA).

Western blot

Lung tissue samples were lysed with the RIPA lysis buffer (Sigma, St. Louis, MO, USA). The protein concentration was measured by the Dc protein assay (Bio-Rad, Hercules, CA). An 80 μg/well of protein was separated on 8–16% gradient SDS-PAGE gels (i.e., Tris-based electrophoresis using standard Laemmle's method) and transferred to a PVDF membrane. Proteins were detected either with commercially available anti-spike antibody at 1:100 dilution and anti-β-actin antibody at 1:2500 dilution as a loading control. Western blot (WB) images were acquired using the Azure cSeries 600 system and auto-exposure settings (Azure Biosystems, CA).

Ethics

Experimental animal protocol No. 04/B042021 was reviewed by and approved in 2021 by the Animal Care and Use Committee at the Dr Rath Research Institute.

Statistical analysis

Data for all experiments, unless indicated otherwise, are presented as an average value and SD from at least three independent experiments, each at least in three replicates. Comparison between different samples was done by a

two-tailed T-test using the Microsoft Office Excel program. Differences between samples were considered significant at p values less than 0.05.

RESULTS

In vivo study using engineered SARS-CoV-2 virons

The overall scheme of the steps completed in the *in vivo* study with engineered SARS-CoV-2 and human HCoV-229E virus, respectively, is presented in Fig. 1. The results presented on Fig. 2 demonstrate the outcomes of the experiment performed with engineered SARS-CoV-2 and show that oral administration of MixV in K18-hACE2 mice caused a mild significant weight change in infected animals, i.e., after 3 days post infection (dpi), and no weight change in re-infected with rVSVΔG-SARS-CoV-2-S-D614Gd21-NLucP virions mice, i.e., after 5 dpi (Fig. 2A). Figure 2B instead concludes that the viral loads in lung samples of infected mice that were on oral administration of MixV

decreased by 1.2 $\log_{10}$ at 3 dpi and subsequently was lower by 0.6 $\log_{10}$ at 5 dpi, compared to their representative controls. Interestingly, we noticed about 1.1 $\log_{10}$ lower viral load in lung samples of control animals collected at 5 dpi versus the lung samples collected at 3 dpi. Viral burden in lung tissue was determined by RT-qPCR and is represented as VSV L gene copies normalized to mouse Pol2Ra. The presence of spike protein followed a similar trend as observed with viral load. As shown on Fig. 2C about 32.4% decrease in spike protein level was noticed in samples from mice infected and treated with MixV on 3 dpi compared to its control, and about 21.2% decrease in samples gathered from animals infected and treated with MixV on 5 dpi compared to its control. Again, control samples acquired on 5 dpi have about 17.9% lower amount of spike protein compared to control samples of animals collected on 3 dpi.

Histologic analysis of the lung tissue and immunohistochemistry evaluation for the presence of spike protein in mice taking MixV is presented in Fig. 3. The results on the upper panel show changes in H&E lung structure with infection and re-infection, whereas results on the lower panel represent immunochemical staining against SARS-CoV-2 protein in pulmonary tissue of mice. Their analysis revealed that infected and re-infected mice developed pulmonary pathology that encompassed the presence of perivascular leukocytes, hyaline membrane, and edema. Also, lung tissue of MixV-gavaged mice had noticeably lower degree of pathology compared to control infected mice especially around pulmonary vasculature with less alveolar and peribronchiolar disease manifestation. Interestingly, re-infection did not meaningfully worsen this picture. Immunostaining for SARS-CoV-2 spike protein revealed its more prevalent distribution in infected untreated animals compared to more curbed distribution in MixV-gavaged animals. Again, presence of detected SARS-CoV-2 spike
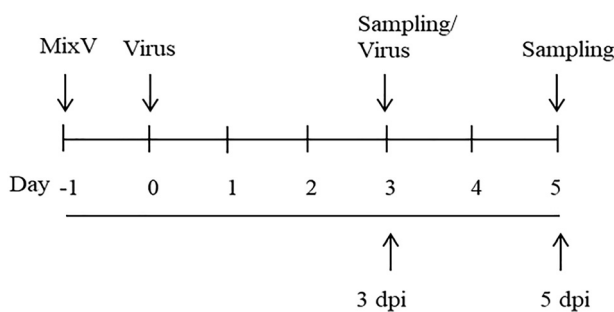

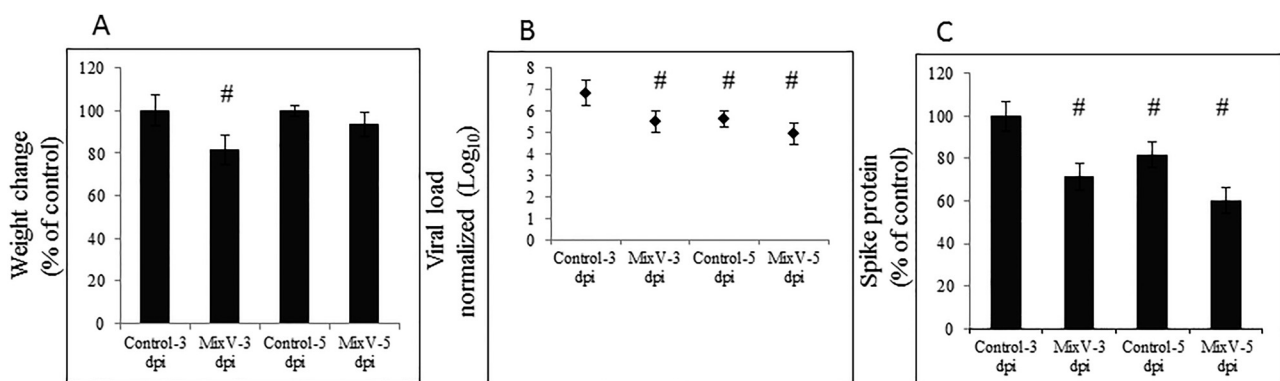Fig. 1. **Scheme representing the experimental design**, dpi - days post-infection

Fig. 2. **Effect of the test composition on weight change, viral load and spike protein in lung tissue in mice infected with rVSVΔG-SARS-CoV-2-S-D614Gd21-NLucP virion and after re-infection**. A. Effect of four-day gavaging of MixV in K18-hACE2 mice with observed weight change and six-day of gavaging of MixV in K18-hACE2 mice, which were mid-term re-infected with no observed weight change after five days of infection. B. Decrease in viral load ($\log_{10}$) in infected lung tissue in mice consuming MixV after 4 days (3 dpi) and 6 days (5 dpi) with re-infection on third day by the same virus. The decrease was expressed by $\log_{10}$ compared to respective controls. C. Decrease in spike protein in the mice lungs after consuming MixV for 4 and 6 days with re-infection with the same virus on third day. Quantification of SARS-CoV-2 spike protein in mice lungs was performed as described in Materials and Methods. Data are presented as mean ± SD; infected untreated animal $n = 8$, infected treated animal $n = 8$, re-infected untreated animal $n = 8$, re-infected treated animal $n = 8$, #$P \leq 0.05$, dpi - days post-infection
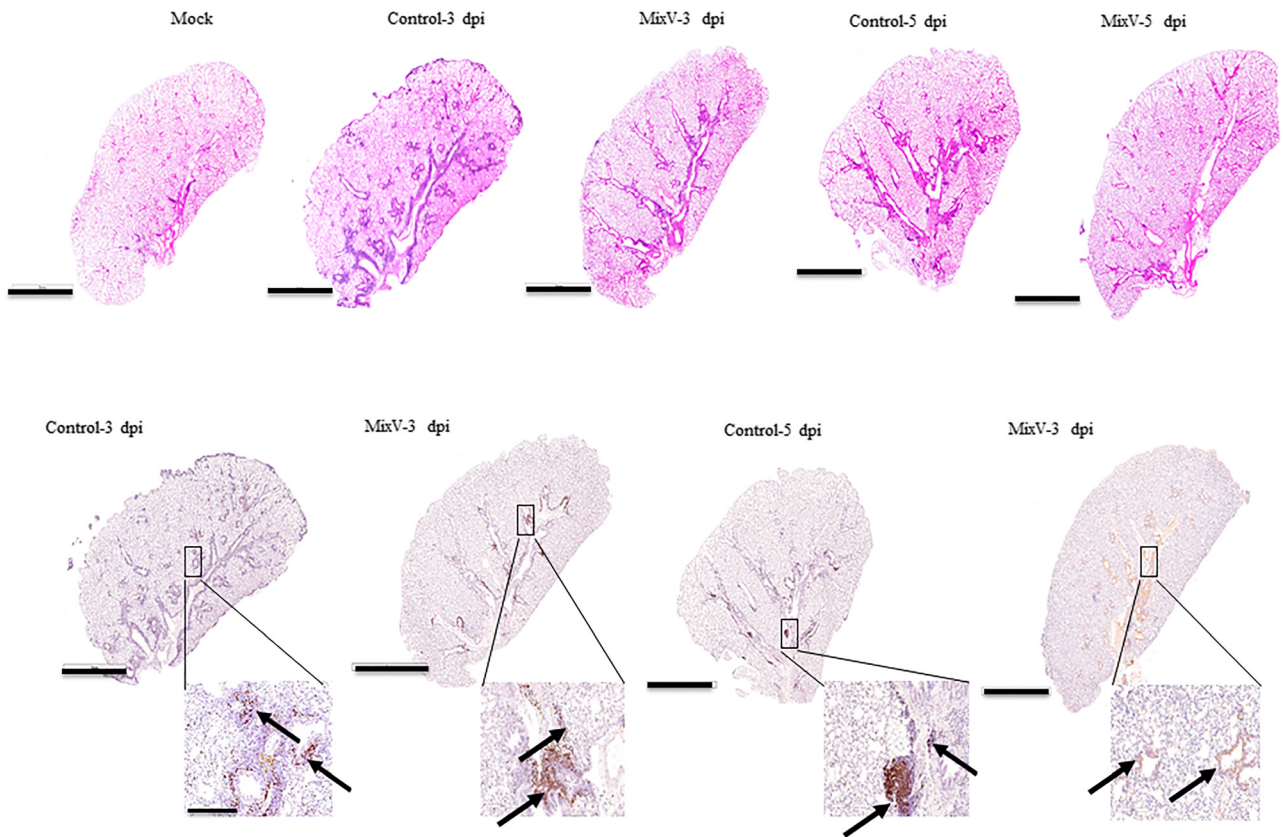
Fig. 3. **Effect of the test composition on histological changes in the lung tissue after rVSVΔG-SARS-CoV-2-S-D614Gd21-NLucP virion infection and re-infection**. Representative photomicrographs of *in vivo* experiment where rVSVΔG-SARS-CoV-2-S-D614Gd21-NLucP virion were used. Upper panel show H&E staining whereas lower panel presents detection of spike protein in lung tissue on 3 dpi and 5 dpi. Quantification of anti-spike protein antibody was performed as described in Materials and Methods section. Mock animals $n = 2$, infected untreated animal $n = 8$, infected treated animal $n = 8$, re-infected untreated animal $n = 8$, re-infected treated animal $n = 8$, scale bar = 3 mm and 200 μm; dpi – days post-infection, arrow – positive staining

protein in re-infected animals compared to infected animals was less revealing.

Analysis of H&E-stained and Spike-CoV-2 protein-stained lung sections from 3 dpi and 5 dpi animals indicated an inflammatory process similar to the one previously reported [16]. Further, immunochemical staining against CD11b (i.e., pan myeloid cells) that have been shown to correlate with disease severity in patients with COVID-19 was significantly lower by about 26.2% in MixV-gavaged mice for four days compared to control and by about 19.3% in MixV-gavaged mice for six days compared to respective control (Fig. 4A and B). This analysis also showed a 17.1% decrease in CD11b-positive cells in the non-treated and re-infected animals compared to non-treated and only-once-infected animals.

Additionally, the levels of cytokines TNFα, IL1β, ILα, and IL17 in the BAL was also significantly lower in those infected mice that were MixV-treated for five days compared to its respective untreated infected control (Fig. 4C). Also, in BAL from the lung of infected mice collected on 5 dpi, compared to infected mice collected on 3 dpi, lower level of IL10 and similar level of TNFα and IL17 were found. In addition, our experiment with SARS-CoV-2 VPLs showed

that activation of NF-κB decreases to the level similar to control (i.e., unstimulated cells) in cells treated with MixV (Fig. 4D).

In vivo study using HCoV-229E virus

Figure 5 presents the results of the experiment performed with human HCoV-229E virus and shows that the weight of mice gavaged with MixV underwent slight non-statistical change on 3 dpi compared to its representative control (Fig. 5A). Interestingly, re-infection did not have a significant impact on body weight. Viral load in the lungs decreased about 1.3 $\log_{10}$ on 3 dpi compared to its representative control (Fig. 5B). Also, in control mice re-infected on a third day there was about 0.7 $\log_{10}$ decrease in viral load in the lung tissue samples collected on 5 dpi compared to respective controls. Moreover, in obtained control samples from 5 dpi, a 1.2 $\log_{10}$ decrease was observed compared to control samples collected on 3 dpi. The presence of spike protein paralleled the pattern observed for a viral load with about 43.3% decrease on 3 dpi compared to the control (Fig. 5C and D). Re-infection resulted in reduced spike level by about 27.6% compared to the control. Re-infected control
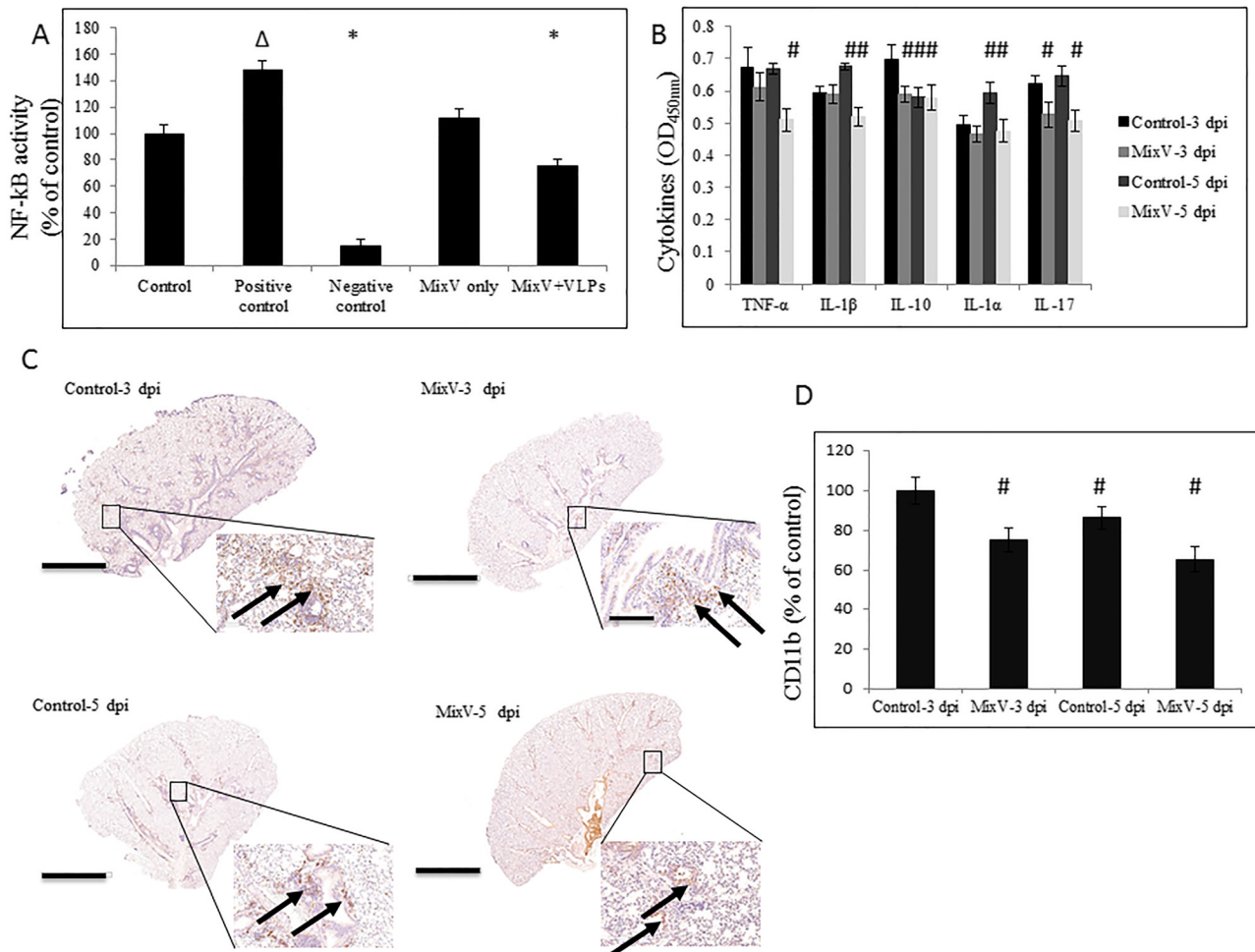
Fig. 4. **Effect of the test composition on inflammatory response in vitro and *in vivo*.** A. Effect of MixV on NF-κB activity, where reporter cells were treated with $10 \, \mu g \, ml^{-1}$ concentration of MixV and stimulated with SARS-CoV-2 VLPs. Activity was assessed using NF-κB activity ELISA kit after 24 h post-treatment. B. Effect of MixV on cytokines level in BAL of K18-hACE2 mice after 4 days of administration or 6 days of oral administration with mid-term re-infection. The cytokines level was assessed with ELISA as described in Materials and Methods section. C. Effect of MixV on CD11b antibody level in lung sections of orally gavaged mice for 4 days and orally gavaged mice for 6 days, with mid-term re-infected. D. Quantification of CD11b antibodies was performed as described in Materials and Methods section. Data are presented as mean ± SD; infected untreated animal $n = 8$, infected treated animal $n = 8$, re-infected untreated animal $n = 8$, re-infected treated animal $n = 8$, scale bar = 3 mm and 200 μm; #$P \leq 0.05$, Δ $P \leq 0.01$, *$P \leq 0.001$, dpi - days post-infection, BAL - bronchoalveolar lavage, VLPs - viral like particles, arrow – positive staining

mice samples from 5 dpi also had lower spike protein level by 14.5% compared to the level of spike protein detected in control mice on 3 dpi.

DISCUSSION

Current approaches against SARS-CoV-2 infection, including the vaccines, have limited applications since their high specificity requires frequent adjustments to the rapidly mutating virus. In search of a more universal approach, we turned to micronutrients, which as natural compounds, have a capacity to simultaneously affect multiple cellular mechanisms. Our earlier report indicated that a specific combination of vitamins, polyphenols, and other natural ingredients (i.e., MixV) can be effective in inhibiting key

cellular mechanisms associated with SARS-CoV-2 infection *in vitro*, including its variants [11–15]. Here we evaluated the efficacy of this composition *in vivo* using K18-hACE2 C57BL/6J mice infected with rVSVΔG-SARS-CoV-2-S-D614Gd21-NLucP virions (as a suricate for SARS-CoV-2) and also a seasonal coronavirus HCoV-229E. In regards to SARS-CoV-2 virus, our experiment was limited by the use of rVSVΔG-SARS-CoV-2-S-D614Gd21-NLucP virions characterized by lower infectivity. These virions, however, are replication-competent and infectious, thus suitable for BSL2+ laboratories. The engineered SARS-CoV-2 virions used are appropriate for *in vivo* experiments to study pulmonary pathologies, especially with respect to inflammatory response, as we previously showed as well [16].

Overall, our results show that a short-term (i.e., four days) administration of MixV caused the decrease of viral
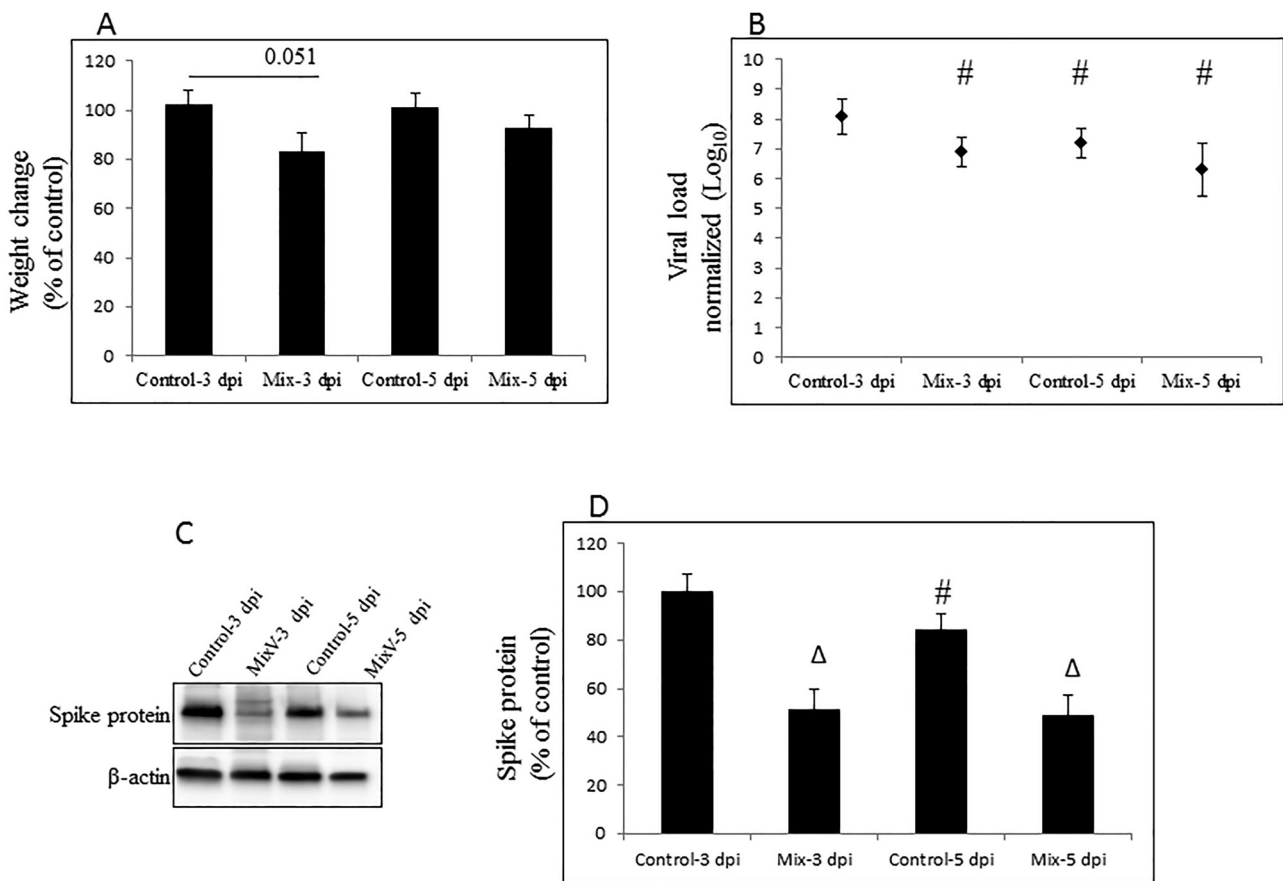
Fig. 5. **Effect of test composition on weight change, viral load and spike protein in lung tissue infected and re-infected with human coronavirus 229E (HCoV-229E)**. A. Effect of four-days of oral administration of MixV in K18-hACE2 mice with no significant weight change after 3 dpi and 5 dpi and oral administration of MixV with mid-term re-infection. B. The viral load in lung tissue after 3 dpi with oral administration of MixV and 5 dpi with oral administration and mid-term re-infection, determined by RT-qPCR as described in Materials and Methods section. C. Spike protein detection by WB in representative lung tissue samples. D. Quantification of spike protein performed as described in Materials and Methods section. Data are presented as mean $\pm$ SD; infected untreated animal $n = 8$, infected treated animal $n = 8$, re-infected untreated animal $n = 8$, re-infected treated animal $n = 8$; #$P \leq 0.05$, Δ $P \leq 0.01$, dpi - days post-infection

load and spike protein level in the lungs of mice infected with SARS-CoV-2 virions. A similar inhibiting effect was observed in mice that were re-infected and gavaged. Analogous response patterns were observed when mice were infected or re-infected with HCoV-229E seasonal coronavirus resulting in decreased viral load and levels of spike protein in the lung tissue. Significantly, these inhibiting effects were similar or even greater than those reported for remdesivir in a similar mouse model [17]. We found it interesting that there were fewer viral particles detected in the lung tissue of re-infected animals compared with lungs of animals infected only once. A similar observation of decreased viral load and peribronchial and perivascular inflammation was reported with the original SARS-CoV-2 virus as well [17]. This could be wholly or partially influenced by innate and/or humoral responses, which in turn is facilitated by the viral spike protein.

Our *in vivo* results confirm a significantly reduced viral replication and viral-triggered inflammation in the lungs of infected mice treated with MixV. They also reaffirm a decreased presence of infiltration with CD11b (pan-myeloid cells) that were acknowledged as initiators and maintaining factors of lung inflammatory process associated with SARS-CoV-2 infection [17–21]. This recruitment of blood monocytes into the lung has been also recognized as an 'initiator and keeper' of pulmonary inflammatory responses in other lung diseases such as ARDS [21].

One consistent outcome observed in our *in vivo* studies was that mice consuming MixV responded similarly in decreasing viral load and spike protein in the lungs infected and re-infected with HCoV-229E and rVSVΔG-SARS-CoV-2-S-D614Gd21-NLucP. This would suggest that the MixV was not specific to one type of coronavirus but rather affected common mechanisms of coronavirus infectivity.

Both our *in vitro* and *in vivo* studies showed that application of MixV was effective in decreasing pro-inflammatory cytokines. Since inflammation is the leading factor in SARS-CoV-2-triggered lung injury, our findings are of particular significance. In both, initial infection and subsequent re-infection, the levels of CD11b antibodies in the lungs of mice infected with HCoV-229E and rVSVΔG-SARS-CoV-2-S-D614Gd21-NLucP virus decreased to a

similar degree. This was accompanied by decreased cytokines levels in BAL samples as well as NF-κB activity *in vitro*.

MixV evaluated in this study contains natural compounds with strong antioxidant, anti-inflammatory, and viral metabolic pathways modulating properties as the basis of wide specificity and pleiotropic efficacy. In our earlier study we showed that among 56 natural compounds evaluated, brazilin, theaflavin-3,3′-digallate (TF3), and curcumin had the highest binding ability with the RBD of spike protein, thereby inhibiting viral attachment to the human ACE2 and thus cellular entry of pseudo-typed SARS-CoV-2 virions [22]. In addition, TF3 and curcumin inhibited activity of TMPRSS2 and cathepsin L proteases that facilitate the binding and endosomal egress of SARS-CoV-2 virus. Quercetin revealed its anti-viral efficacy as well by interfering with various stages of the SARS-CoV-2 entry and replication cycle affecting PLpro, 3CLpro, and NTPase/helicase [23]. The antiviral properties of baicalin tested both *in vitro* and *in vivo* showed its modulatory activity against viral protein NS1, resulting in up-regulation of IFN signaling, and a decrease in PI3K/Akt pathway [24]. Another compound, resveratrol, is strong antioxidants with an anti-inflammatory effect inhibiting of NF-κB pathway. Its anti-viral effects also include inhibitions of viral replication, protein synthesis, gene expression, and nucleic acid synthesis as reported by Nayak et al. [25]. Sulforaphane (SFN), the principal biologically active phytochemical of broccoli extract, was shown *in vitro* to inhibit replication of six strains of SARS-CoV-2, including Delta and Omicron variants. Prophylactic administration of SFN to K18-hACE2 mice prior to intranasal SARS-CoV-2 infection significantly decreased the viral load in the lungs and upper respiratory tract reducing lung injury and pulmonary pathology as well [26]. These data in addition to our own evaluations indicated complementary anti-SARS-CoV-2 effects of these natural compounds' combinations [14].

Nonetheless, all this scientific evidence warrants further medical evaluation regarding suitability of their application in clinical settings. SARS-CoV-2 infection, as well as many other pathologies, are often a result of multiple extracellular and intracellular factors, so it may be too optimistic to assume that targeting one mechanism will eradicate the problem. Using one natural compound even in high amounts does not always fully address the complexity of metabolic problem, as illustrated by clinical application of vitamin C in high doses in COVID-19 patients as well [27–29]. However, such efficacy may be enhanced by complementary nutrients. Our research confirms the potential value of this combination of natural compounds in simultaneously inhibiting various key pathways of coronavirus infectivity. In this aspect, we have also shown earlier that those individual components, e.g., ascorbic acid, which has been clinically applied in high doses in COVID-19 patients [29], can significantly decrease cellular expression of ACE2 receptors at the protein and RNA levels. Its efficacy can also be potentiated by combining it with other micronutrients and phytochemicals (i.e., zinc, epigallocatechin-3-gallate) [13–15].

Towards this, our research reaffirms the value of simultaneously targeting key metabolic pathways of SARS-CoV-2, its mutants and seasonal coronavirus infectivity by administering a combination treatment and addressing complex metabolic pathologies. While each ingredient displays distinct metabolic specificity, their synergistic and complementary interactions allow for increased efficacy and simultaneous expansion of cellular mechanisms affected. In addition, application of natural compounds as multi-nutrient combinations also allows achieving desired results with lower doses of individual compounds compared to their use as separate ingredients. A lack of, or negligent side effects of, natural compounds are also beneficial for their potential application in preventive and therapeutic aspects of infection.

ACKNOWLEDGMENT

REFERENCES

1. Weekly epidemiological update on COVID-19 - 22 February 2023. World Health Organization. https://www.who.int/publications/m/item/weekly-epidemiological-update-on-covid-19—22-february-2023.

2. Moore JP, Offit PA. SARS-CoV-2 vaccines and the growing threat of viral variants. JAMA 2021;325(4):301–2. PMID: 33512449. https://doi.org/10.1001/jama.2021.1114.

3. Cao Y, Yisimayi A, Jian F, Song W, Xiao T, Wang L, et al. BA.2.12.1, BA.4 and BA.5 escape antibodies elicited by Omicron infection. Nature 2022;608(7923):593–602. https://doi.org/10.1038/s41586-022-04980-y.

4. Cao Y, Wang J, Jian F, Xiao T, Song W, Yisimayi A, et al. Omicron escapes the majority of existing SARS-CoV-2 neutralizing

antibodies. Nature 2022;602(7898):657–63. https://doi.org/10.1038/s41586-021-04385-3.

5. Wang Q, Guo Y, Iketani S, Nair MS, Li Z, Mohri H, et al. Antibody evasion by SARS-CoV-2 Omicron subvariants BA.2.12.1, BA.4 and BA.5. Nature 2022;608(7923):603–8. https://doi.org/10.1038/s41586-022-05053-w.

6. Cele S, Jackson L, Khoury DS, Khan K, Moyo-Gwete T, Tegally H, et al. Omicron extensively but incompletely escapes Pfizer BNT162b2 neutralization. Nature 2022;602(7898):654–6. https://doi.org/10.1038/s41586-021-04387-1.

7. Tuekprakhon A, Nutalai R, Dijokaite-Guraliuc A, Zhou D, Ginn HM, Selvaraj M, et al. Antibody escape of SARS-CoV-2 Omicron BA.4 and BA.5 from vaccine and BA.1 serum. Cell 2022; 185(14):2422–2433.e13. https://doi.org/10.1016/j.cell.2022.06.005.

8. Dejnirattisai W, Huo J, Zhou D, Zahradník J, Supasa P, Liu C, et al. SARS-CoV-2 Omicron-B.1.1.529 leads to widespread escape from neutralizing antibody responses. Cell 2022;185(3):467–484.e15. https://doi.org/10.1016/j.cell.2021.12.046.

9. Wang K, Jia Z, Bao L, Wang L, Cao L, Chi H, et al. Memory B cell repertoire from triple vaccinees against diverse SARS-CoV-2 variants. Nature 2022;603(7903):919–25. https://doi.org/10.1038/s41586-022-04466-x.

10. Cele S, Gazy I, Jackson L, Hwa SH, Tegally H, Lustig G, et al. Escape of SARS-CoV-2 501Y.V2 from neutralization by convalescent plasma. Nature 2021;593(7857):142–6. https://doi.org/10.1038/s41586-021-03471-w.

11. Goc A, Niedzwiecki A, Ivanov V, Ivanova S, Rath M. Inhibitory effects of specific combination of natural compounds against SARS-CoV-2 and its Alpha, Beta, Gamma, Delta, Kappa, and Mu variants. Eur J Microbiol Immunol (Bp) 2022;11(4):87–94. https://doi.org/10.1556/1886.2021.00022.

12. Goc A, Rath M, Niedzwiecki A. Composition of naturally occurring compounds decreases activity of Omicron and SARS-CoV-2 RdRp complex. Eur J Microbiol Immunol (Bp) 2022;12(2):39–45. https://doi.org/10.1556/1886.2022.00009.

13. Ivanov V, Ivanova S, Niedzwiecki A, Rath M. Effective and safe global public health strategy to fight the COVID-19 pandemic: specific micronutrient combination inhibits Coronavirus cell-entry receptor (ACE2) expression. J Cell Med Nat Health 2020;July. https://jcmnh.org/index.php/2020/07/02/effective-and-safe-global-public-health-strategy-to-fight-the-covid-19-pandemic-specific-micronutrient-composition-inhibits-coronavirus-cell-entry-receptor-ace2-expression/.

14. Ivanov V, Goc A, Ivanova S, Niedzwiecki A, Rath M. Inhibition of ACE2 expression by Ascorbic acid alone and its combination with other natural compounds. Infect Dis (Auckl) 2021;14, 1178633721994605. https://doi.org/10.1177/1178633721994605.

15. Goc A, Sumera W, Ivanov V, Niedzwiecki A, Rath M. Micronutrient combination inhibits two key steps of coronavirus (SARS-CoV-2) infection: viral binding to ACE2 receptor and its cellular expression. J Cell Med Nat Health 2020;August. https://jcmnh.org/index.php/2020/08/14/micronutrient-combination-inhibits-two-key-steps-of-coronavirus-sars-cov-2-infection-viral-binding-to-ace2-receptor-and-its-cellular-expression/.

16. Goc A, Sumera W, Rath M, Niedzwiecki A. Linoleic acid binds to SARS-CoV-2 RdRp and represses replication of seasonal human coronavirus OC43. Sci Rep 2022;12, 19114. https://doi.org/10.1038/s41598-022-23880-9.

17. White KM, Rosales R, Yildiz S, Kehrer T, Miorin L, Moreno E, et al. Plitidepsin has potent preclinical efficacy against SARS-CoV-2 by targeting the host protein eEF1A. Science 2021;371(6532):926–31. https://doi.org/10.1126/science.abf4058.

18. Jiang RD, Liu MQ, Chen Y, Shan C, Zhou YW, Shen XR, et al. Pathogenesis of SARS-CoV-2 in transgenic mice expressing human angiotensin-converting enzyme 2. Cell 2020;182(1):50–58.e8. https://doi.org/10.1016/j.cell.2020.05.027.

19. Winkler ES, Bailey AL, Kafai NM, Nair S, McCune BT, Yu J, et al. SARS-CoV-2 infection of human ACE2-transgenic mice causes severe lung inflammation and impaired function. Nat Immunol 2020;21(11):1327–35. https://doi.org/10.1038/s41590-020-0778-2.

20. Oladunni FS, Park JG, Pino PA, Gonzalez O, Akhter A, Allué-Guardia A, et al. Lethality of SARS-CoV-2 infection in K18 human angiotensin-converting enzyme 2 transgenic mice. Nat Commun 2020;11(1):6122. https://doi.org/10.1038/s41467-020-19891-7.

21. D'Alessio FR, Heller NM. COVID-19 and myeloid cells: complex interplay correlates with lung severity. J Clin Invest 2020;130(12): 6214–7. https://doi.org/10.1172/JCI143361.

22. Goc A, Sumera W, Rath M, Niedzwiecki A. Phenolic compounds disrupt spike-mediated receptor-binding and entry of SARS-CoV-2 pseudo-virions. PLoS One 2021;17;16(6): e0253489. https://doi.org/10.1371/journal.pone.0253489.

23. Agrawal PK, Chandan Agrawal Ch, Blunden G. Quercetin: antiviral significance and possible COVID-19 integrative considerations. Nat Prod Commun 2020;15(12):1–8. https://doi.org/10.1177/1934578X209762.

24. Moghaddam E, Teoh BT, Sam SS, Lani R, Hassandarvish P, Chik Z, et al. Baicalin, a metabolite of baicalein with antiviral activity against dengue virus. Sci Rep 2014;26(4):5452. https://doi.org/10.1038/srep05452.

25. Nayak M, Agrawal SS, Bose S, Naskar S, Bhowmick R, Chakrabarti S, et al. Antimicrob Chemother 2014;69(5):1298–310. https://doi.org/10.1093/jac/dkt534.

26. Ordonez AA, Bullen CK, Villabona-Rueda AF, Thompson EA, Turner ML, Merino VF, et al. Sulforaphane exhibits antiviral activity against pandemic SARS-CoV-2 and seasonal HCoV-OC43 coronaviruses in vitro and in mice. Commun Biol 2022;18;5(1):242. https://doi.org/10.1038/s42003-022-03189-z.

27. Thompson EA, Cascino K, Ordonez AA, Zhou W, Vaghasia A, Hamacher-Brady A, et al.. Metabolic programs define dysfunctional immune responses in severe COVID-19 patients. Cell Rep 2021; 34(11): 108863. https://doi.org/10.1016/j.celrep.2021.108863.

28. Mishra P, Pandey N, Pandey R, Tripathi YB. Role of macrophage polarization in acute respiratory distress syndrome. J Respiration 2021;1(4):260–72. https://doi.org/10.3390/jor1040024.

29. Zhang J, Rao X, Li Y, Zhu Y, Liu F, Guo G, et al. Pilot trial of high-dose vitamin C in critically ill COVID-19 patients. Ann Intensive Care 2021;11(1):5. https://doi.org/10.1186/s13613-020-00792-3.